COMPOSITES & POLYCON 2009
American Composites Manufacturers Association
January 15-17, 2009
Tampa, FL USA

Fiber Reinforced Cementitious Matrix Composites for Infrastructure Rehabilitation

by

Francisco J. De Caso y Basalo
Fabio Matta
Antonio Nanni

Department of Civil, Architectural, and Environmental Engineering, University of Miami

Abstract

The use of externally-bonded fiber reinforced polymer systems for confinement of reinforced concrete columns has become an accepted practice to increase the strength and ductility. This paper reports on early results of a research program aimed at developing an innovative class of externally bonded composite systems that use cement-based matrices. The overarching goal is to develop and validate sustainable, compatible and reversible cement-based composite strengthening systems.

The focus of this paper is on the first, completed task of the program, which was aimed at assessing the feasibility of the research project. Specifically, work was conducted to: a) address constructability; and b) provide evidence of the adequacy of a cementitious-matrix with compatible fiber architecture.

Once the optimal mix design was selected for three candidate cementitious matrices, a total of fifteen 152 mm (6 in.) diameter concrete cylinder specimens were wrapped using two-ply continuous reinforcement schemes. The installation procedure resembled that typical of the wet-layup technique used for epoxy-based systems. The specimens were tested under pure axial compression load. Constructability and compatibility issues were overcome, as the strengthened specimens exhibited a noticeable increase in both strength and axial deformation at failure. Ongoing research is focusing on the refinement of the technology, and on the use of alternative fiber material systems.

1. Introduction

The use of externally-bonded fiber-reinforced polymer (FRP) systems to rehabilitate existing reinforced concrete (RC) structures has been developing rapidly, and an appreciable number of RC bridges, buildings and structures have been strengthened, repaired and retrofitted around the world. Furthermore, design guidelines and recommendations have been published [1-3].

Externally-bonded FRP systems are effectively implemented in seismic areas, where performance must comply with increasingly demanding design codes; as well as non-seismic areas, typically due to deterioration, insufficient reinforcement, higher load demand, or change in use. The use of FRP jackets to enhance strength and deformability of RC columns has become an accepted practice, mainly due to cost-benefit advantages that draw from ease and speed of application and minimal invasivity. In addition, FRP confinement increases the shear resistance of columns and prevents premature spalling failures due to lateral loadings such as those experienced during earthquakes.

Despite the advantages of conventional FRP systems, there are other desirable features that could extend the application of these systems on RC structures. First is the issue of economics, which is to increase the availability of lower cost materials, both reinforcing fibers and polymeric resins. Second are technological issues, related to the use of organic polymeric resins as matrices: in a fire event these resins will fuel the fire and toxic fumes will be released, which can damage the biological system of potentially trapped humans. Further elementary issues relating to the organic resins include, the potential hazard to workers during application, non-applicability on wet surfaces or at low temperatures, low vapor permeability (which may cause damage to the concrete structure being strengthened), need for strict quality control, susceptibility to UV radiation and low reversibility.

The project reported herein aims at providing a response to some of these limitations by developing innovative and sustainable externally-bonded strengthening systems that use inorganic matrices. This paper reports on the first completed task with the objective of validating the feasibility of the systems, using glass fiber reinforcement embedded in a cement-based matrix, herein referred to as fiber reinforced cementitious matrix (FRC) composites. The goal of the feasibility study was to address the requirements of constructability and compatibility of the fiber/matrix system for RC column confinement applications.

2. Background and Research Significance

Fiber reinforced mortars (FRM) [4], have been part of the construction industry for a long period of time. Though the mechanics of cementitious based matrices for fiber reinforced composites was explored during the 1970s, with intrinsic models developed [5], no direct confinement applications were devised. Though slow progress was made – it was not until the 1990s – developments for permanent forms for new construction [6] and rehabilitation [7-8] were made, with an emphasis on applications for shear and/or flexural strengthening [9-10]. Recent studies [11-14] have concluded in their findings that organic matrices can be as effective as inorganic ones for composite strengthening in flexural, shear and confinement applications, thus showing the capability of inorganic matrices versus organic ones. Further research is being undertaken to study the use of textile/mesh type reinforcement instead of fiber sheets for concrete confinement, showing that significant increases in compressive strength and deformation capacity can be attained [15-17]. A field application using a fiber glass mesh embedded in a cement-based matrix for the seismic strengthening of all dome roofs of the Basilica of Santissima Annunziata in Sicily [18] shows the versatility of inorganic matrices and their potential for implementation.

Sustainable construction requires a critical review of prevailing practices, economics, techniques, materials and their sources. Focus is turning towards natural and compatible systems, and the idea of an FRC system is a candidate fulfilling these requirements, as well as providing a response to some limitations of FRP systems. These inorganic matrices when applied on concrete or masonry surfaces have a high degree of chemical and mechanical compatibility. Additional compelling features are thermal stability, non-flamability, resistance to UV radiation, and ease of handling and safety, since grouts are water-based products and emit no odor or toxins, which reduce health and safety risks during fire events.

3. Experimental Program

The experimental program was developed with three main purposes: 1) to explore different types of grouts as inorganic matrices along with different types of fiber architecture; 2) to assess constructability of the candidate strengthening systems; and 3) to evaluate system compatibility and effectiveness by testing confined concrete cylinders in pure compression.

A total of 15 concrete cylinders, 152 mm (6 in.) diameter and 305 mm (12 in.) in height, were wrapped with two plies of fiber reinforcement, along with 3 control (unwrapped) specimens. The cylinders were cast from a single batch and left to cure for 28-days, yielding an average strength of 23.2 MPa (3370 psi) after testing in accordance with ASTM C 39, as reported in Table 1.

3.1 Materials selection

3.1.1 Fiber Architecture

Two types of glass fiber architecture were used (sheet and mesh), and a total of three different fiber reinforcements comprised the test matrix:

a) Sheet-architecture (Unidirectional)
   - *i. S560: low density glass fiber sheet* 560 g/m^2 (15.5 oz/yd^2)
   - *ii. S915: high density glass fiber sheet* 915 g/m^2 (27.0 oz/yd^2)

b) Mesh-architecture (Bi-directional)
   - iii. *M250:* 250 g/m^2 (7.5 oz/yd^2)

The sheet architecture was chosen based on the typical fiber density of 600 g/m^2 (18.0 oz/yd^2) for glass fiber sheets used in confinement applications. Two density limits were considered, namely: a low density fiber-sheet (Figure 1) with a tensile strength of 420 MPa (60.4 ksi) and a high density fiber-sheet (Figure 2) with a tensile strength of 3240 MPa (470 ksi). The alkaline-resistant mesh/textile type of reinforcement (Figure 3), characterized by a mean tensile strength of 45 kN/m (0.26 kip/in), was selected since previous literature has shown this architecture type to be a viable option. Each fiber roving in the 90° direction was 2.67 mm (0.105 in.) wide and in the 0° there were two rovings, each 1.96 mm (0.077 in.) wide. The clear spacing between rovings in the 90° direction was 20.27 mm (0.798 in.) and in the 0° 22.50 mm (0.886 in.).

3.1.2 Grout – Inorganic Resin

The main parameters considered for the grouts used as cement-based matrices were based on their ability to: a) permeate the fibers and reach an adequate degree of "wettability", thus requiring relatively fine based grouts; b) provide sufficient bond strength: though confinement is a contact-critical application, the need to bond with the concrete substrate is necessary to transfer load to the fibers, ensuring that good contact is maintained while the grout cures with the reinforcing fibers; c) allow sufficiently curing time to ensure workability when preparing the samples; and d) ensure dimensional stability.

Three different grouts were selected:

- *i. Grout type-A:*

Two part acrylic-modified Portland cement based matrix, which creates a flexible breathable matrix.

ii. *Grout type-H:*
Hydraulic cement-based matrix with high water retention, extreme fine aggregate and paste rich, yielding a cohesive grout.

iii. *Grout type-M:*
Single component magnesium-phosphate-based matrix, with a 15-minute setting time and good bonding capability without an added bonding agent. This product contains coarse grain particle size, which was sieved and re-formulated to agree with the established parameter of a fine based grout.

Refer to Table 2 for the grout compressive strengths (ASTM C109) and Table 3 for tensile split strengths (ASTM D3967).

3.2 Specimen preparation

Two individual specimens were prepared with each fiber reinforcing architecture and grout combination. The fiber/matrix configurations are summarized in the first column of Table 1. The notation of the specimens is in the format X000_B_C, where X refers to the fiber architecture type (Control: C, Sheet: S, or Mesh: M), followed by for the density of the fiber in g/m^2, while B denotes the grout type used as matrix (Type A, H or M) and C indicates the specimen number (1 or 2).

3.2.1 Percentage of liquid by weight of powder
The need to select the most desirable liquid by weight of powder ratio for individual grouts was undertaken first. This lead to an iterative process, where a two-fold intention was to produce a grout that, 1) was fluid enough to saturate fibers, while at the same time, 2) have the viscosity to hold the fiber reinforcement onto the surface of the concrete cylinder, while vertically hardening without sliding. It is important to note that each grout had different mixing ratios due to their independent characteristics, which are summarized in Table 2, resulting in plastic consistency and good workability. The grouts were prepared and tested according to ASTM C109, after curing for 7 days.

3.2.2 Constructability
In order to ensure ease for field implementation of this strengthening system, the procedure used to wrap the continuous reinforcing fibers around the cylinders resembled that typical of wet lay-up techniques used for epoxy-based systems. The fabrication procedure for specimens is documented in Figure 4 to Figure 8. Application of the inorganic matrix was simple and straight forward while attaching a continuous two-ply tensile reinforcement. Impregnation of the fibers was enhanced through the use of a ribbed roller. As observed, this technique yielded a positive outcome due to appropriate grout viscosity, bonding to the substrate while holding the fiber reinforcement in place.

3.3 Testing procedure

Specimens were left to rest at room conditions, 23.8°C (75°F) and 65% R.H, allowing the grout to harden for 7 days. The specimens were capped with rubber caps and tested under displacement control, at a rate of 0.254 mm/min (0.015 in/min) using a 890 kN (200 kip) capacity test frame.

4. Test Results and Discussion

The results are rendered in the form of representative normalized stress-strain graphs (Figure 9, Figure 10 and Figure 11) with respect to the ultimate stress and strain of a representative control specimen. The results of this preliminary experimental stage indicated that:

a) It was possible to evaluate adequate materials – both fiber architecture types and matrix grouts – for the composite strengthening systems.
b) Compatible strengthening systems were recognized.
c) The strengthening systems based on fibers embedded in inorganic matrices were verified to be feasible, showing increases in strength and significantly enhanced deformability.

4.1 Hydraulic binders

During the determination of the ratios of liquid by weight of powder of the grouts, it was apparent that grouts type A and H had the right consistency and characteristics to impregnate all types of fiber architectures while bonding to the concrete surface. These results are summarized in Table 2 and show the following:

At 45% of liquid (acrylic) ratio grout type-A, yielded an optimal workability with a slightly adhesive-like consistency. Performance-wise, this grout had a relatively low mean compressive strength of 2.46 MPa (356.8 psi) compared to type-H, and even lower average tensile strength of 0.20 MPa (29.6 psi) at 7 days. This was probably due to the acrylic component that yielded a plastic like matrix, as noticed in the failure mode of the cubes (Figure 12). A ductile behavior was observed, as the sides of the cube deformed and curved outwards after failure with no spalling (Figure 12).

On the other hand, grout type-H, at only 27% of water ratio, had relatively higher fluidity than type-A. This grout reached a high compressive strength, 30.58 MPa (4435.8 psi) and tensile strength 1.47 MPa (213.4 psi) failing in shear as traditional brittle mortars (Figure 13). Both hydraulic binders were able to bond to the substrate during preparation of the specimens, holding the fiber in place. The only exception was with fiber M250, embedded in type-H grout, the ratio was too fluid for the architecture type. Though the fiber remained attached to the substrate, as the grout cured, a significant amount slipped vertically as seen in Figure 14**Error! Reference source not found.**. Additionally, voids between the fiber, grout and cylinder surface were noticeable, not providing the continuity needed for confinement effect. Specimens M250_H_1 &_2 were not tested.

Grout type-M at only 11% became fluid enough to permeate through the fibers. However even though the coarse aggregates were sieved out, it was possible to feel through handling of the grout, that the remaining particles were still too large to penetrate the fibers. Furthermore, the behavior of type-M grout was comparable to quicksand, when inducing stresses (handling it) it had the appropriate workability; otherwise, its consistency became less fluid and not compatible with any fiber reinforcement as seen in Figure 15**.** As a consequence, this grout was not able to be implemented as part of a strengthening system, since preparation of satisfactory specimens was not possible.

4.2 Low density FRC system – S560

Representative normalized stress-strain graphs during the pure axial compressive tests of cylinders wrapped in the S560 reinforcing fibers (low density fiber sheets) are provided in Figure 9.

The graphs are characterized by a bi-linear trend: the first branch ascending closely to the slope of the control specimen (unconfined), followed by the second branch, which for the specimen with matrix grout-A (acrylic-modified grout), is close to horizontal; dropping suddenly when the jacket failed by rupture due to hoop stresses. The second branch for matrix grout-H (hydraulic-based grout), is also ascending, however at a lower slope than the initial branch, which also ends with a sudden drop. Specimens did provide a noticeable increase in peak strength: 16% with type-A grout and 34% with type-H. Figure 9 also shows the significant increase in ultimate strain (relative to the control), which is of equal magnitude for samples with both types of grouts. All samples engaged showing external fissure patterns with different types of matrix failure. Matrix grout type-A (Figure 16), engaged as it slipped and stretched without spalling over the tensile reinforcement, while transferring load. On the other hand, matrix grout type-H (Figure 17) fully engaged as the concrete expanded laterally after cracking, exerting tension on the matrix which failed locally where the fibers ruptured after reaching the ultimate strain. Notice that even though the fibers embedded in grout type-H reached their full strength due to rupture, the specimens did not reach a higher ultimate strain compared to samples embedded in grout type-A, where fibers did not rupture. However the ultimate strength was higher when grout type-H was used, this is most likely due to the hydraulic grout's ability to permeate the fiber since it is water-based, instead of acrylic-modified. Overall, it can be concluded that the fiber-inorganic matrix combination yields a significant enhancement in deformability and some strength increase.

4.3 High density FRC system – S915

Figure 10 shows the characteristic normalized stress-strain graphs for samples reinforced with S915 fiber sheets, embedded in grout types-A and H, as well as the control specimen (unwrapped).

As seen in Figure 10 the graphs for the samples with grout type-H follow a similar bi-linear response as observed with the low density FRC system (S560). This is also true for specimens with matrix grout type-A, with a second quasi-horizontal branch ascending slightly till sudden failure. Literature has shown that high density fiber reinforcing sheets may not provide useful increases in ultimate strength due to the inability of the resin to fully impregnate the fibers, thus negatively affecting compatibility. This was experienced in samples with grout type-A, which yielded an average of 10% reduction in ultimate strength using high density S915 fibers, versus using low density S560 fibers. On the other hand, no reduction was observed when matrix grout type-H was used, and resulted in a 40% increase in ultimate strength (close to the 34% when using low density fibers). This reflects that grout type-H has a higher wetting capability compared with grout type-A, which has an acrylic-base.

In contrast, ultimate strain for both grouts with S915 fibers remained the same, such as those with specimens using S560 fibers. The failure mechanisms for specimens with matrix grout type-H resembled those experienced with S560 fibers, reaching rupture of the matrix and fibers (Figure 19). On the contrary, samples with grout type-A had no surface fissures (Figure 18), and looked unchanged after testing. This lack of failure pattern on tested specimens may have been caused due to low impregnation of the fibers by grout type-A.

4.4 Mesh fiber reinforcement system

The only successful composite system with the M250 fiber architecture was the one embedded with matrix grout type-A. Figure 11 shows the normalized stress-strain relationship for a representative sample. It can be seen that this type of fiber architecture provides only limited ultimate strength and strain increase. Figure 20 shows specimen M250_A_1 after testing, no appreciable failure patterns on the matrix can be noticed, illustrating that the tensile reinforcement did not transfer any load. This is likely due to the stiffness that the tensile reinforcement mesh self-contained. During the specimen construction the fiber mesh tended to coil outwards while wrapping it around the cylinder – due to the small wrapping-radius – hence disrupting continuity between the matrix and the fibers.

4.5 Scanning electron microscope

Scanning Electron Microscope (SEM) was implemented to better understand the degree of compatibility of the composite systems: 1) at the interface between the concrete substrate and the matrix and 2) at the fiber sheet ply/matrix interfaces, which shows the level of impregnation.

Figure 21 shows the interface between the substrate and the first layer of matrix grout type-A. It is appreciable that there is good continuity and bonding, similar to grout type-H. As expected, the level of impregnation for both fiber architectures was low as illustrated in Figure 22, which shows the individual rovings of the low density fiber sheet were only partially impregnated by the matrix. In some cases, individual rovings at scattered locations had extremely low degree of impregnation as noticed in Figure 23, which illustrates an individual roving in the low density glass fiber sheet (S560) and the acrylic based grout. Figure 23 can also explain the type of slipping failure modes experienced with grout type-A.

4.6 Validation: initial results

Initial validation results in the form of stress-strain graphs illustrated in Figure 24 and Figure 25, have revealed further considerable increase levels of ultimate strength and strain for the fiber reinforced cementitious-based strengthening composite system – FRC, with both type of grouts curing after 28-days. All cylinders were cast from a single batch and left to cure for 28-days, yielding an average strength of 20.4 MPa (2958 psi) and ultimate strain of 2598 με. Figure 26 shows the test setup under pure axial compression used for the validation of the FRC strengthening system. Load measurements were made through a 1379MPa (200 kip) capacity load cell, and axial-strain by using four displacement transducers (pi-gauges) attached to two rings connected to the specimen. Furthermore four direct current differential transducers (DCVTs) were used to measure the transverse deformations.

Figure 24 shows the stress-strain behavior for representative specimens wrapped with the low density (S560) glass fiber sheet. It is interesting to point out that the behavior of samples with either grout type is comparable in strength as both provide a significant increase. In terms of deformability, the levels of strain have greatly increased in comparison to the control (unwrapped) specimen. Samples with the acrylic modified grout (type-A) reached a higher strain of approximately 10100 με, than those with the hydraulic modified grout (type-H) at around 8300 με.

Initial stress-strain results for representative specimens confined with the high density (S915) glass fiber sheets are illustrated in Figure 25. A gradual drop in post-peak strength was observed up to a significant strain level. On the other hand, the increase in ultimate strength for samples with grout type-A was significantly reduced. There was a remarkable behavior in terms of deformability, where samples reached an ultimate strain of around 21600 με. For samples with matrix grout type-H, the peak strain was reached at 10700 με.

These initial results reflect that after further curing of the matrix grout, bonding is substantially increased. This creates an improved load transfer to the fiber reinforcement, which yields significant strength increase and deformability enhancement.

5. Conclusions

The results of the feasibility study reported herein indicated that compatibility issues and constructability for cement-based matrix composite systems for RC column confinement were successfully addressed. The composite systems tested produced noticeable increases in both strength and deformability of concrete cylinders. The use of fiber architecture with clear spacing between individual rovings, such as the low density glass fiber sheet, allowed for a more effective impregnation. This architecture type was the most effective reinforcement with both types of acrylic and hydraulic cementitious matrices, with higher levels of ultimate strength reached with the hydraulic based grout and similar levels of ultimate strain. Additional results from the ongoing testing campaign have shown that considerable increases in strength and ultimate strain may be attained with both types of fiber glass sheet reinforcement.

Acknowledgments

The authors would like to acknowledge the financial support of the National Science Foundation Industry/University Cooperative Research Center for Repair of Buildings and Bridges with Composites (RB^2C). The contribution of materials from Mapei and BASF is gratefully acknowledged as well as Phil Davis at the Dauer Electron Microscopy Lab, University of Miami.

Authors

Francisco J. De Caso y Basalo is a Graduate Research Assistant at the Department of Civil, Architectural, and Environmental Engineering at the University of Miami. His research focuses on the use of sustainable advanced composite material systems for concrete repair and rehabilitation.

Fabio Matta is a Research Assistant Professor at the Department of Civil, Architectural, and Environmental Engineering at the University of Miami. His research interests include the use of advanced materials for the internal and external reinforcement of concrete.

Antonio Nanni is the Lester and Gwen Fisher Endowed Scholar, Professor and Chair at the Department of Civil, Architectural, and Environmental Engineering at the University of Miami. His research interests include the evaluation, repair and rehabilitation of concrete structures.

References

1. American Concrete Institute, ACI 440.2R-08, Guide for the Design and Construction of Externally Bonded FRP Systems for Strengthening Concrete Structures, Reported by ACI Committee 440, 2008.
2. The concrete society, Technical Report 55: Design guidelines for strengthening concrete structures using fibre composite materials, 2nd edition, Cambertey, 2004.
3. A. Mirmiran, M. Shahawy, A. Nanni, V. Karbhari, National Cooperative Highway Research Program Report 514, "Bonded Repair and Retrofit of Concrete Structures Using FRP Composites", 2004
4. M. A. Taylor, M. K. Tai, and M. R. Ramey "Biaxial Compressive Behavior of Fiber Reinforced Mortar",., ACI Journal Proceedings, Vol 72, Issue 9, pp 496-501, September 1975.
5. J. Aveston, G. A. Cooper, and A. Kelly, Conference on the Properties of Fibre Composites, pp 15-26, IPC Science and Technology Press, Guildford, Surrey, 1971.
6. Y. Sato, S. Fujii, Y. Seto, and T. Fujii, "Structural Behavior of Composite Reinforced Concrete Members Encased by Continuous Fiber-Mesh Reinforced Mortar Permanent Forms", American Concrete Institute, Farmington Hills, MI, pp. 113-124, 1999.,
7. W. Dolan, S. H. Rizkalla, and A. Nanni, "Fiber Reinforced Polymer Reinforcement for Reinforced Concrete Structures", American Concrete Institute, Farmington Hills, MI, , pp. 113-124, 1999.
8. P. Balaguru, and S. Kurtz, "Use of Inorganic Polymer-Fiber Composites for Repair and Rehabilitation of Infrastructures", Procedings of Repair and Rehabilitation of Reinforced Concrete Structures, pp.155–168, 1997.
9. J. I. Daniel, and S. P. Shah, "Thin-Section Fiber Reinforced Concrete and Ferrocement", SP-124, American Concrete Institute, Farmington Hills, MI, pp. 441, 1990.
10. A. Foden, R. Lyon, P. Balaguru, and J. Davidovitz, "High Temperature Inorganic Resin for use in Fiber Reinforced Composites", Procedings 1st International Conference on Composites in Infrastructures, University of Arizona, Tucson, AZ, pp. 166–177, 1996.
11. R. Garon, P. Balaguru, and H. Toutanji, "Performance of Inorganic Polymer-Fiber Composites for Strengthening and Rehabilitation of Concrete Beam", Procedings 5th International Conference on Fiber-Reinforced Plastics for Reinforced Concrete Structure, Vol. 1, pp. 53–62, 2001.
12. S. Kurtz, and P. Balaguru, "Comparison of Inorganic and Organic Matrices for Strengthening of RC Beams with Carbon Sheets", Journal of Structural Engineeing, Vol. 127, No. 1, pp. 35–42, 2001.
13. H. C. Wu, and J. Teng, "Concrete Confined with Fiber Reinforced Cement Based Thin Sheet Composites", FRPRCS-6 Fiber Reinforced Polymer Reinforcement for Concrete Structures, 2006.
14. H. Toutanji, and Y. Deng, "Comparison between Organic and Inorganic Matrices for RC Beams Strengthened with Carbon Fiber Sheets", Journal of composites for construction September, 2007.
15. T. C. Triantafillou, and C. G. Papanicolaou, "Textile Reinforced Mortars (TRM) versus Fiber Reinforced Polymers (FRP) for Concrete Confinement", ConMat'05 and Mindess Symposium, Construction Materials, N. Banthia, T. Uomoto, A. Bentur, and S. P. Shah, University of British Columbia, BC, Canada, 2005.
16. T. C. Triantafillou, C. G. Papanicolaou, P. Zissimopoulos, and T. Laourdekis, "Concrete Confinement with Textile-Reinforced Mortar Jackets", ACI Structural Journal, Vol. 103, No. 1, pp. 28-37, 2006.

17. D. A. Bournas, P. V. Lontou, C. G. Papanicolaou, and T. C. Triantafillou, "Textile-Reinforced Mortar versus Fiber-Reinforced Polymer Confinement in Reinforced Concrete Columns", ACI Structural Journal, Vol. 104, No. 6, 2007.
18. G. Morandini, Build Dossier http://www.infobuilddossier.it/view_approfondimenti.php?id=69&id_dossier=42, Accessed October, 24 2007.

Figures:

Figure 1 - S560, low density glass fiber sheet (inch scale).

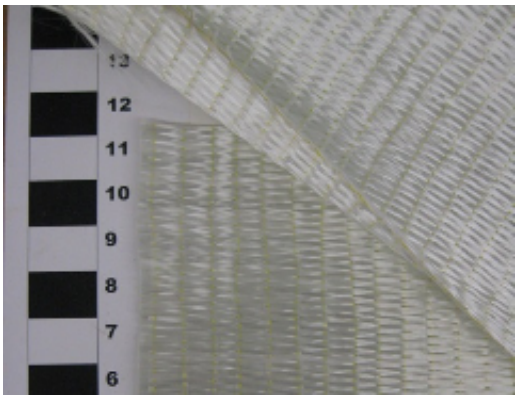

Figure 2 - S915, high density glass fiber sheet (inch scale).

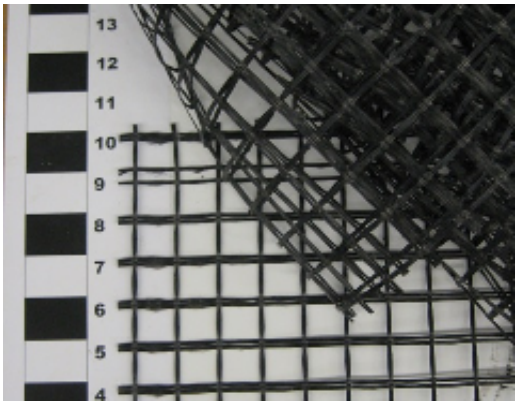

Figure 3 - M250, glass mesh/textile (inch scale).

Figure 4 - Application of substrate.

Figure 5 - Knife edge and start of fiber wrapping.

Figure 6 - Embedding fiber with ribbed roller.

Figure 7 - Application of grout.

Figure 8 - Finished Specimen.

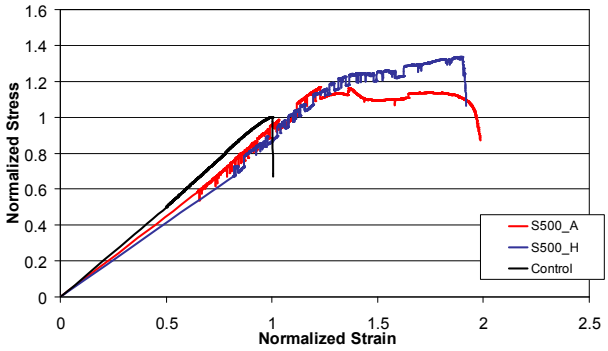

Figure 9 - Normalized Stress-Strain for representative samples with S560 reinforcing fibers.

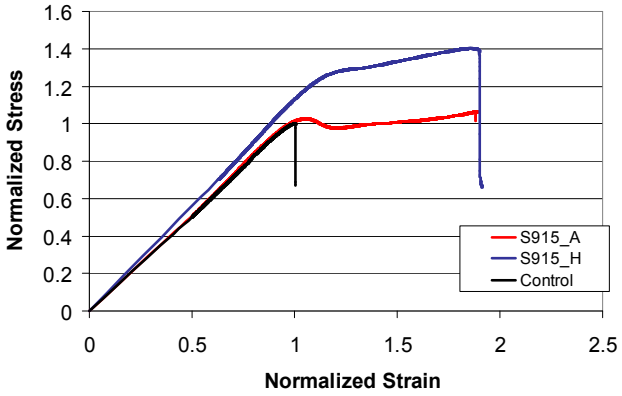

Figure 10 - Normalized Stress-Strain for representative samples with S950 reinforcing fibers.

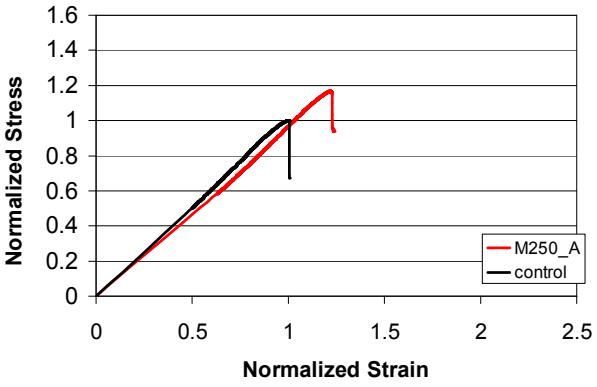

Figure 11 - Normalized Stress-Strain for representative samples with M250 reinforcing fibers.

Figure 12 - Compression failure of grout type-A.

Figure 13 - Compression failure of grout type-H.

Figure 14 (Left) - Specimen M250_H_1.

Figure 15 (Right) - Specimen S560_M_1.

Figure 16 (Left) - Specimen S560_ A_1.

Figure 17 (Right) - Specimen S560_H_1.

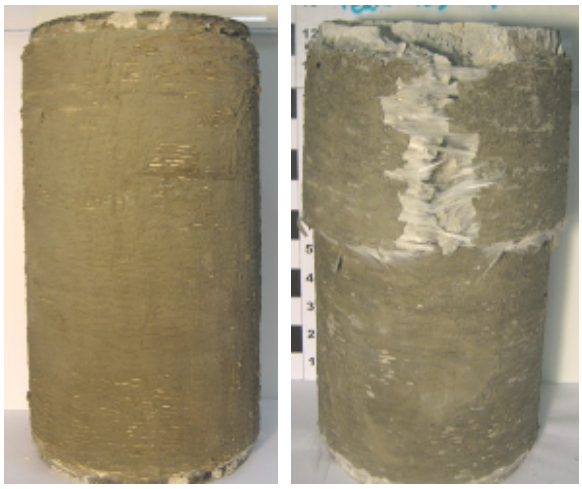

Figure 18 (Left) - Specimen S915_ A_1.
Figure 19 (Right) - Specimen S915_ H_1.

Figure 20 - Specimen M250_A_1.

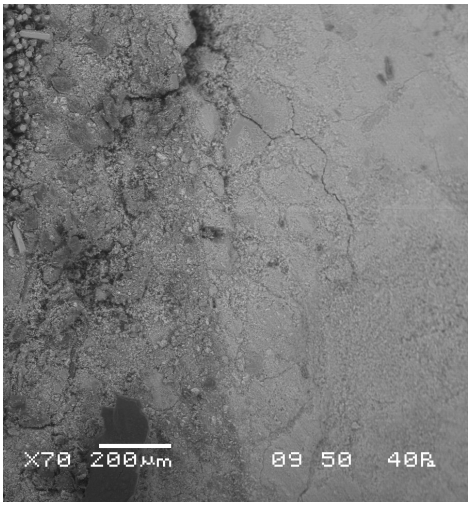

Figure 21 - SEM image specimen G500_A_1: first matrix layer (left) – substrate (right).

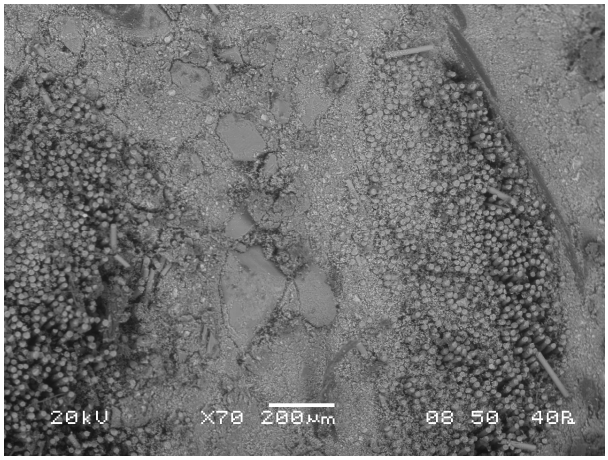

Figure 22 - SEM image specimen G500_A_1 (left to right): 2nd ply - matrix - 1st ply - first layer of matrix.

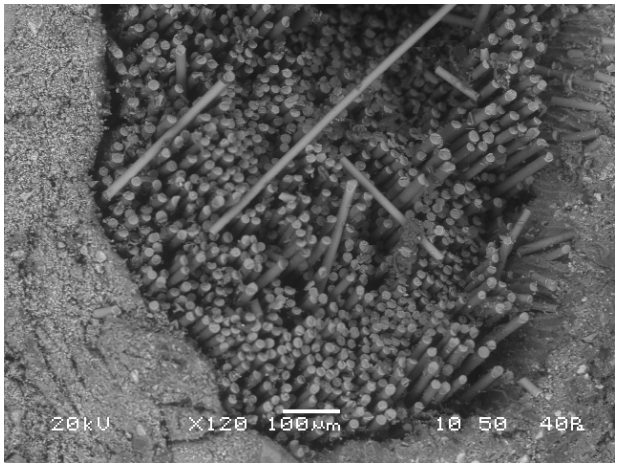

Figure 23 - SEM image: single roving.

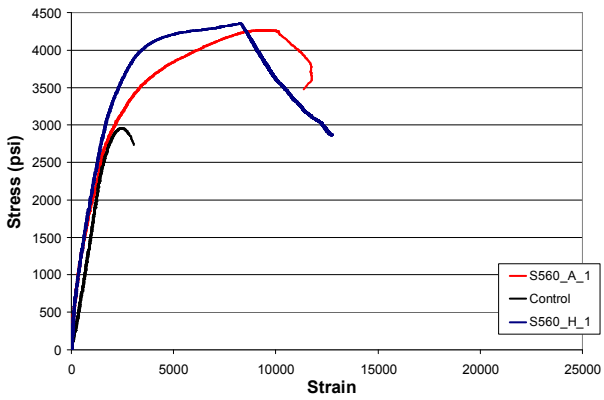

Figure 24 - Stress-Strain graph for samples strengthen with low density glass fiber sheet.

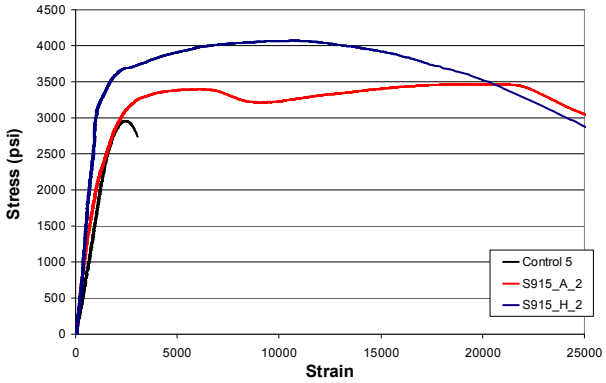

Figure 25 - Stress-Strain graph for samples strengthen with high density glass fiber sheet.

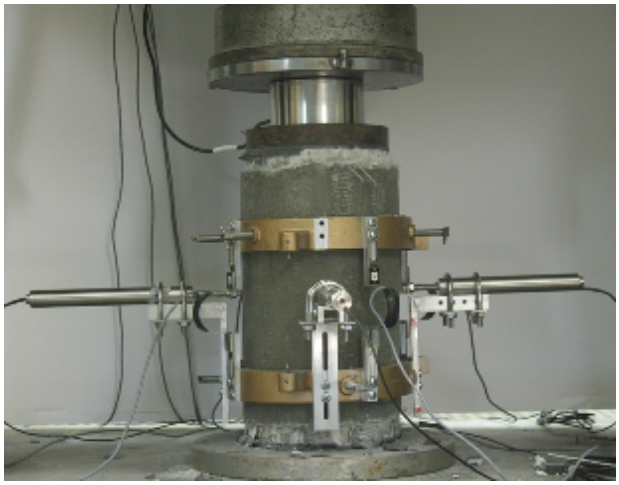

Figure 26 - Test setup for validation of the FRC strengthening composite system.

Specimen notation	Compressive strength		Peak Norm. Stress	Peak Norm. Strain
	psi	MPa		
C_1	3197	22.04		
C_2	3517	24.25		
C_3	3395	23.41		
S560_A_1	3998	27.56	1.19	1.60
S560_A_2	3735	25.75	1.11	1.98
S560_H_1	4273	29.46	1.27	1.93
S560_H_2	3734	25.75	1.11	1.45
S915_A_1	3413	23.53	1.01	1.91
S915_A_2	3799	26.19	1.13	1.76
S915_H_1	4212	29.04	1.25	1.88
S915_H_2	4481	30.90	1.33	1.91
M250_A_1	3728	25.70	1.11	1.24
M250_A_2	3386	23.34	1.00	1.26

Table 1 - Strength and normalized ultimate stress and strain of specimens

Grout	Liquid weight of powder	Peak load (lbs)	Comp. strength (psi)	Mean Compressive strength (psi)	MPa
Type-A	45 %	1247	311.8	356.8	2.46
		1504	376.0		
		1530	382.5		
Type-H	27 %	17420	4355.0	4,435.8	30.58
		16080	4020.0		
		19730	4932.5		

Table 2- Specific mixing ratios for grouts and compressive strength

Grout	P (lb)	L (in)	D (in)	Splitting tensile strength (psi)	(MPa)
Type-H	2250	4	2	179.0	1.23
Type-H	3390	4	2	269.8	1.86
Type-H	2320	4	2	184.6	1.27
Type-H	2450	4	2	195.0	1.34
Type-H	3000	4	2	238.7	1.65
		AVERAGE		**213.4**	**1.47**
Type-A	370	4	2	29.4	0.20
Type-A	400	4	2	31.8	0.22
Type-A	350	4	2	27.9	0.19
Type-A	380	4	2	30.2	0.21
Type-A	360	4	2	28.6	0.20
		AVERAGE		**29.6**	**0.20**

Table 3 - Splitting tensile Strength of grout